Proposal to Jefferson Lab PAC 24

Probing the Limits of the Standard Model of Nuclear Physics with the ^{4}He$(\vec{e}, e'\vec{p})^3$H Reaction

N. Benmouna, B.L. Berman, B. Briscoe, G. Feldman, Y. Ilieva,
S. Strauch (spokesperson)
The George Washington University, Washington, DC

R. Gilman, C. Glashausser, X. Jiang, G. Kumbartzki, K. McCormick,
R.D. Ransome (co-spokesperson)
Rutgers University, Piscataway, NJ

J. Arrington
Argonne National Laboratory, Argonne, IL

C.F. Perdrisat
College of William and Mary, Williamsburg, VA

R. Ent (co-spokesperson), D.W. Higinbotham, M.K. Jones, D.G. Meekins,
B. Reitz
Jefferson Lab, Newport News, VA

V. Punjabi
Norfolk State University, Norfolk, VA

C.E. Hyde-Wright, P.E. Ulmer (co-spokesperson), L.B. Weinstein
Old Dominion University, Norfolk, VA

F. Butaru, S. Choi, Z.E. Meziani, K. Slifer, P. Solvignon, H. Yao
Temple University, Philadelphia, PA

J.R.M. Annand, D. Hamilton, D.G. Ireland, J.D. Kellie, K. Livingston,
D. Protopopescu, G. Rosner, D.P. Watts
University of Glasgow, Glasgow, United Kingdom

J.J. Kelly
University of Maryland, College Park, MD

and the Hall A Collaboration

Abstract

We propose high precision measurements of the double ratio of polarization transfer coefficients, P'_x and P'_z, of the quasielastic $^4\mathrm{He}(\vec{e}, e'\vec{p})\,^3\mathrm{H}$ reaction with respect to the elastic $^1\mathrm{H}(\vec{e}, e'\vec{p})$ reaction, at a Q^2 of 0.8 (GeV/c)^2 and 1.3 (GeV/c)^2. Recently, measurements of this double ratio at both Mainz and JLab hinted at the need to include medium modifications of the proton form factors predicted by a quark-meson coupling model. The proposed experiment would reduce the statistical uncertainties in the double polarization ratio at each Q^2 by over a factor of two compared to the previous measurement, resulting in roughly equal contributions from statistical and systematic uncertainties. These two Q^2 values were selected since they lie in a region where theoretical calculations are expected to be reliable. This measurement would provide one of the most stringent tests to date of the applicability of conventional meson-nucleon calculations.

1 Physics Motivation

1.1 Introduction

The underlying theory of strong interactions is Quantum ChromoDynamics (QCD), yet there are no ab-initio calculations of nuclei available. Nuclei are effectively and well described as clusters of protons and neutrons held together by a strong, long-range force mediated by meson exchange, whereas the saturation properties of nuclear matter arise from the short-range, repulsive part of the strong interaction [1]. At nuclear densities of about 0.17 nucleons/fm^3 nucleon wave functions have significant overlap. In the chiral limit, one expects nucleons to lose their identity altogether and nuclei to make a transition to a quark-gluon plasma. This phase transition is extensively being studied at the RHIC facility.

Whether the nucleon bound in the nuclear medium changes structure has been a long-standing issue in nuclear physics. The discovery of the nuclear EMC effect almost twenty years ago brought the subjects of quarks into nuclear physics with great impact. However, the specific causes of the modifications observed in nuclear structure functions have not yet been identified with certainty [2]. Any medium modification of bound nucleon form factors carries implications for the nuclear EMC effect [3]. For example strong constraints on models of the nuclear EMC effect are placed by model independent relations derived on the basis of quark-hadron duality, which relate the medium modification of the electromagnetic form factors to the modification of the deep-inelastic structure function of a bound proton [4].

Within QCD there is no known way to derive anything like an atomic nucleus in which the constituents do not change as the mean density (or temperature) goes away from zero [5]. A calculation by D.H. Lu *et al.* [6], using a quark-meson coupling (QMC) model, suggests a measurable deviation from the free space form factor ratio over the Q^2 range $0.0 < Q^2 < 2.5$ (GeV/c)^2. Note that the calculation is consistent with present constraints on possible medium modifications for both the electric form factor (from the Coulomb Sum Rule, with $Q^2 < 0.5$ $(\mathrm{GeV/c})^2$ [7, 8, 9]), and the magnetic form factor (from a y-scaling analysis [10], for $Q^2 > 1$ $(\mathrm{GeV/c})^2$), and limits on the scaling of nucleon magnetic moments in nuclei [11]. Similar measurable effects have been calculated in the light-front constituent quark model of Frank *et al.* [12]. Recently, Yakshiev *et al.* [13] investigated possible modifications to the nucleons' electromagnetic form factors in the ^{4}He nucleus in the framework of a modified Skyrme model, up to $Q^2 = 0.6$ $(\mathrm{GeV/c})^2$. The ^{4}He nucleus is argued to be the lightest nucleus that can be approximated by a continuous matter distribution. The effects are calculated to be small and slightly dependent on the distance of the center of the nucleon from the center of the nucleus. Still, the calculated effects would be accessible by the precision experiment we propose here. Furthermore, the group of G.A. Miller is presently studying medium effects in the framework of a chiral soliton model for the proton [3].

Thus, although models using free nucleons and mesons as quasi-particles are successful in nuclear physics, one may expect that, under certain circumstances, their use is a highly uneconomical approach, especially given that these are not the fundamental entities of the underlying theory. The use of medium-modified nucleons as quasi-particles may be a better choice. To experimentally demonstrate that, it is required to have excellent control of the reaction mechanism effects. The nucleus, as a bound many-body quantum system, has inherent many-body effects, such as meson-exchange currents (MEC) and isobar configurations (IC). In addition, when probing nuclear structure one has to deal with final-state interactions (FSI). A change in the spatial structure of the nucleon, as expressed in medium modifications of the nucleon form factors, implies that one treats observed medium effects as density dependent one-body effects, and assumes that the major part of the many-body effects are therein incorporated. If medium-modified nucleon form factors are defined, in principle medium-modified many body effects are also required in order to perform a rigorous calculation of nuclear structure.

There is no experimental way to distinguish between both approaches: the notion of medium modification of single particle properties like, *e.g.*, the electromagnetic form factors of a nucleon, in a nuclear environment is a purely theoretical concept [14]. Thus, distinguishing possible changes in the spatial structure of nucleons embedded in a nucleus from more conventional many-body effects is only possible within the context of a model. We argue the quasi-elastic proton knockout in the proposed $^4\mathrm{He}(\vec{e}, e'\vec{p}\,)\,^3\mathrm{H}$ reaction to be the most directly accessible experimental method to challenge conventional meson-nucleon calculations where these conventional effects are suppressed.

1.2 Choice of Target

The target nucleus ^{4}He is optimal for further study since its relative simplicity allows for realistic microscopic calculations and since its high density enhances any possible medium effects. Also, a variety of calculations for the $^4\mathrm{He}(\vec{e}, e'\vec{p}\,)\,^3\mathrm{H}$

reaction indicate that polarization transfer observables are influenced little by FSI and MEC effects, amounting to only about a 10% correction [15, 16, 17]. It is precisely these effects (especially FSI) that have so far prevented a clean determination of nucleon medium modifications from unpolarized response functions in $(e, e'p)$ experiments.

If, instead of ^{4}He, one would be able to use a heavier target nucleus, or any nuclear transition, that effectively probes some higher nuclear density region than in the $^4\mathrm{He}(\vec{e}, e'\vec{p}\,)\,^3\mathrm{H}$ reaction, this would be worthwhile. This is illustrated in Fig. 1 [6], showing the calculated dependence on nuclear density in the range of the ^{4}He nucleus. However, in terms of the effective density sampled in the

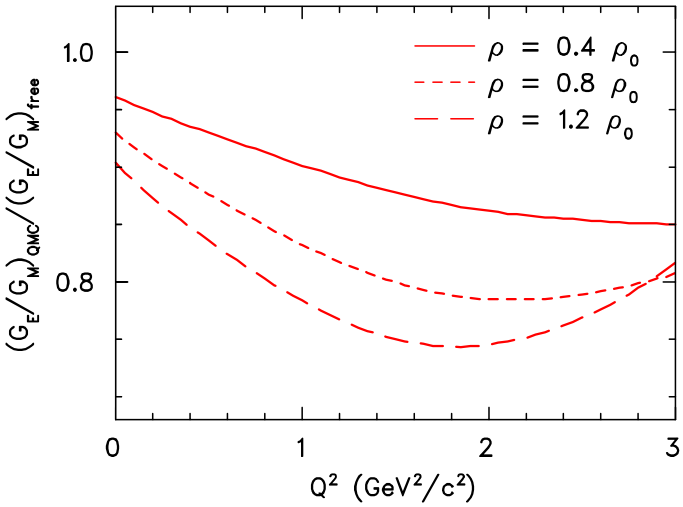

Figure 1: *Ratio of in-medium to free space ratio of electric to magnetic form factors of the proton, for different nuclear densities (in terms of the nuclear matter density ρ_0) [6]. The free bag radius was taken to be 0.8 fm.*

$(e, e'p)$ reaction, ^{4}He is only marginally less dense than heavier nuclei. The average density as sampled in, e.g., the $^{16}\mathrm{O}(e, e'p)$ reaction is only slightly larger than that for the $^4\mathrm{He}(e, e'p)$ reaction (which is about 0.25 times the nuclear matter density), whereas microscopic calculations may be more troublesome, and experimental rates are smaller. Furthermore, Coulomb corrections are more of an issue for heavier nuclei. On the technical side, ^{4}He can easily withstand high beam currents (possible target boiling effects do not affect the double polarization ratio measured). Therefore, ^{4}He remains the target of choice.

1.3 Choice of Reaction

1.3.1 Polarization Transfer

In unpolarized A$(e, e'p)$ experiments involving light- and medium-mass nuclei, deviations were observed in the longitudinal/transverse character of the nuclear response compared to the free proton case [18, 19, 20]. Below the two-nucleon emission threshold, these deviations were originally interpreted as changes in the nucleon form factors within the nuclear medium. However, strong interaction effects on the ejected proton (final state interactions [FSI]) later also succeeded in explaining the observed effect [21]. This illustrates that any interpretation in terms of medium modifications to nucleon form factors requires having excellent control of FSI effects. Still, tantalizing hints of medium effects remain for unpolarized longitudinal/transverse separations in the ^{4}He(e,e$'$p)^{3}H reaction [22, 23].

Polarization transfer in quasielastic nucleon knockout is sensitive to the properties of the nucleon in the nuclear medium, including possible modification of the nucleon form factor and/or spinor. This can be seen from free electron-nucleon scattering, where the ratio of the electric to magnetic Sachs form factors, G_E and G_M, is given by [24]:

$$\frac{G_E}{G_M} = -\frac{P'_x}{P'_z} \cdot \frac{E_e + E_{e'}}{2m_p} \tan(\theta_e/2), \tag{1}$$

where P'_x and P'_z are the transverse and longitudinal transferred polarizations (see [25], and Fig. 9). The beam energy is E_e, the energy (angle) of the scattered electron is $E_{e'}$ (θ_e) and m_p is the proton mass. This relation was recently used to extract G_E/G_M for the proton [26, 27, 28]. For quasielastic nucleon knockout of a bound proton this relation is only approximately correct, but polarization transfer remains sensitive to the properties of the nucleon in the nuclear medium: although proper interpretation of the results requires accounting for such effects as FSI and MEC, their effects on polarization transfer are calculated to be small, as we will demonstrate in the following.

Final State Interactions The majority of studies of the A$(e, e'p)$ reaction have used optical potentials to model FSI. The use of an optical potential for a few-nucleon final state like $p + T$ is somewhat questionable. Lacking a fully microscopic calculation, we address this issue in two ways:

Firstly, a microscopic model developed by Laget was used in successfully describing ^{4}He$(e, e'p)$ data from NIKHEF [32]. Fair agreement was also found between these data and a calculation by Schiavilla using optical potentials [33]. The uncertainty in the latter calculation is associated with the sensitivity of the calculated cross section to the optical potential.

Secondly, our study of the polarization transfer ratio in the ^{4}He$(\vec{e}, e'\vec{p})^3$H reaction demonstrates the insensitivity of the ratio to different optical potentials, shown below. Hence it is likely that details of treatments of FSI do not matter. Within Udias's full relativistic RDWIA model [16] various optical potentials were chosen. Some of the optical potentials we chose were rather extreme, and even in these cases the ratio was insensitive to such choices. Figure 2 compares different acceptance-averaged polarization-transfer double ratios at $Q^2 = 1.0$ (GeV/c)^2 as a function of missing momentum in parallel kinematics, along with the data of the Jefferson Lab experiment "Polarization Transfer in the Reaction ^{4}He$(e, e'p)^3$H in the Quasi-elastic Scattering Region" (E93-049) [29]. The dotted line is the PWIA result. The dashed lines are results of the RDWIA code with six different optical potentials: One group of three is based on RLF folding parameters [30], valid only up to $T_{\rm lab} \approx 400$ MeV, and thus already beyond its regime of validity for Q^2 of 1.0 (GeV/c)^2; the other group of three is based on MRW folding parameters [31]. Each group has one potential based upon the experimental ^{3}H density, one based upon a simple Woods-Saxon density for ^{3}H with the same rms radius as the experimental one, and one with an 30% increased rms radius resulting in an unrealistic potential. It is evident from Fig. 2 that there is hardly any sensitivity in the polarization transfer ratio (within the models examined) to the different choices of optical potentials at low missing momentum.

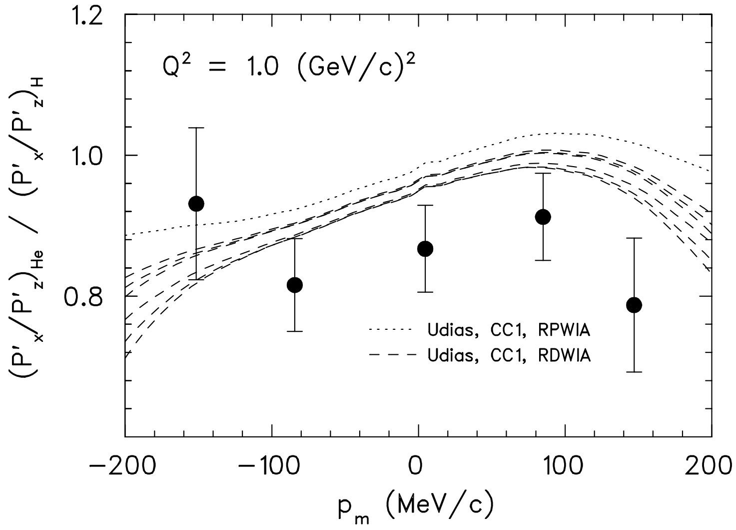

Figure 2: *E93-049 polarization transfer double ratio at $Q^2 = 1.0$ (GeV/c)^2 along with a PWIA and different RDWIA calculations of Udias [16].*

The sensitivity of recoil polarization observables in $A(\vec{e}, e'\vec{p})B$ reactions to channel coupling in final-state interactions was recently investigated by Kelly [34]. Calculations were performed for ^{12}C and ^{16}O. In these studies it was found that polarization transfer observables for proton knockout with modest missing momentum appear to be quite insensitive to details of the final-state interaction, including channel coupling. We estimate the effect of channel coupling for the ^{4}He$(\vec{e}, e'\vec{p})\,^3$H reaction by calculating the relative difference between the polarization transfer ratio with (R_{CC}), and without channel coupling (R). Couplings between the proton $1s_{1/2}$ and neutron $1s_{1/2}$ states were considered. The calculation followed the approach of Kelly [34]. Figure 3 shows the results for a four-momentum transfer of $Q^2 = 1.0$ (GeV/c)^2. The effect is minimal, and on average of the order of 1% – 2%.

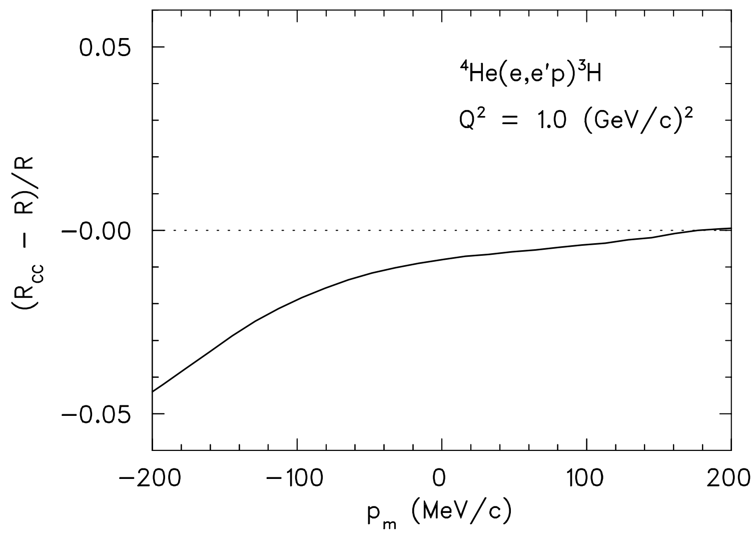

Figure 3: *Relative difference between the polarization transfer ratio including channel coupling, R_{CC}, and without channel coupling, R. The calculation is following the approach of [34].*

MEC and IC Available model calculations indicate that these contributions are smallest in quasielastic, parallel kinematics and at low missing momentum. In a recent work, A. Meucci, C. Guisti, and F.D. Pacati have studied meson-exchange currents in a relativistic model for electromagnetic one-nucleon emission [35]. Meucci has provided us with calculations of the $^4\mathrm{He}(\vec{e}, e'\vec{p})^3\mathrm{H}$ reaction, following the procedures outlined in [35]. Results for the polarization-transfer ratio are shown for the E93-049 kinematics at $Q^2 = 1.0$ (GeV/c)^2 in Fig. 4.

These calculations show that, at low missing momentum, ambiguities due to the choice of the 1-body current ($cc1$, $cc2$, $cc3$) are of the order of 3%; the inclusion of the 2-body current in form of the seagull diagram with one-pion exchange has an asymmetric effect on the polarization ratio about $\mathbf{p}_m = 0$; the effect of MEC reduces the polarization transfer ratio by about 2% on average. In addition, these calculations predict the effect of MEC to decrease with increasing four-momentum transfer (not shown).

We also used the microscopic code of Laget [36] in our analysis of the Mainz and JLab E93-049 data. The result of the full calculation was found to be nearly identical to the PWIA result (see Fig. 6) indicating that reaction mechanisms like MEC, IC, or charge exchange do not contribute significantly in our kinematics. Indeed, "At high momentum transfer, the contribution of many-body and

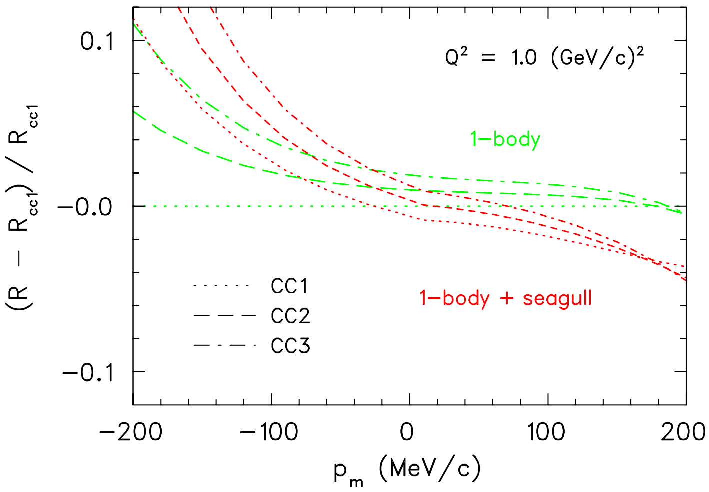

Figure 4: *Calculated polarization-transfer ratios $R = P'_x/P'_z$ relative to R_{cc1} in the $^4He(\vec{e}, e'\vec{p})^3H$ reaction as a function of missing momentum (perpendicular kinematics). Plotted are results for different de Forest current operators with and without the MEC seagull diagram. The 1-body cc1 result serves as baseline. Calculation courtesy of Meucci [35].*

rescattering mechanisms are strongly suppressed and spin observables provide us with a way to study the behavior of the nucleon form factors in the nuclear medium." [36].

1.3.2 Induced Polarization

The induced polarization, P_y, in the $^4\mathrm{He}(e, e'\vec{p})\,^3\mathrm{H}$ reaction is identically zero in the absence of FSI effects (in the one-photon exchange approximation) and constitutes a stringent test of various FSI calculations. A precise knowledge of this quantity will allow improvement of the FSI treatment. Udias even advocates the use of accurate P_y data over elastic $p + T$ scattering data to determine FSI interactions for $(e, e'p)$ experiments. It is thus paramount to accurately determine the value of P_y.

Hence, our approach is to do the best experimental job possible using the $^4\mathrm{He}(\vec{e}, e'\vec{p})\,^3\mathrm{H}$ reaction, in order to put forward as great a challenge as possible for conventional meson-nucleon calculations.

2 Recent Experimental Results

Polarization transfer has been used previously to study nuclear medium effects in deuterium [37, 38, 39]. Within statistical uncertainties, no evidence of medium modifications was found. More recently, polarization-transfer data on $^2\mathrm{H}$ were measured as JLab experiment E89-028 [40], under conditions very similar to those for experiment E93-049 on ^{4}He. Realistic calculations to describe this reaction were performed by Arenhövel [41]. Preliminary experimental results for the ^{2}H-to-^{1}H polarization-transfer double ratio, along with the results of calculations by Arenhövel, are shown in Fig. 5. The full calculation includes FSI, MEC, and IC, as well as relativistic contributions of leading order in p/m to the kinematic wave function boost and to the nucleon current. Arenhövel's full

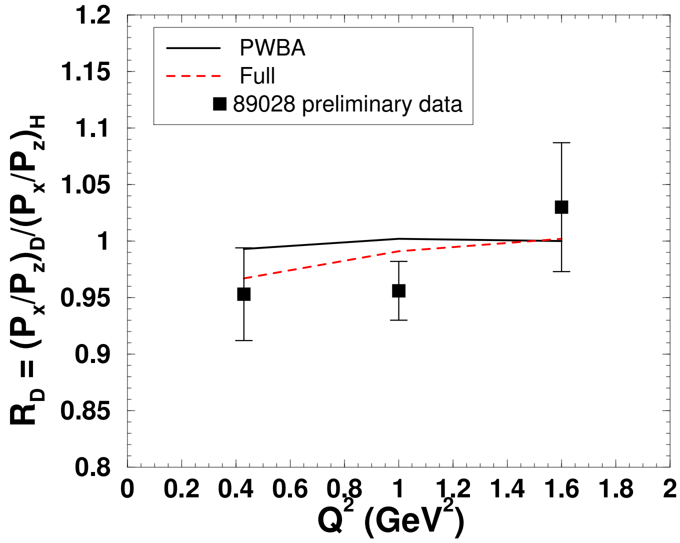

Figure 5: *Polarization transfer double ratio in the $^2H(\vec{e},e'\vec{p})$ reaction; preliminary data from E89-028 along with model calculations from Arenhövel.*

calculation describes the data well. As the sampled density in ^{2}H is signficantly smaller than in ^{4}He, one expects much smaller medium effects in this case, and therefore this agreement is not surprising. Although estimates of the many-body effects in ^{4}He may be more difficult, the calculations mentioned above for ^{4}He indicate they are small.

Recently, polarization transfer in the $^4\mathrm{He}(\vec{e},e'\vec{p})\,^3\mathrm{H}$ reaction at $Q^2 = 0.4$ (GeV/c)^2 was reported [43]. The addition of medium-modified proton form factors, as predicted by the QMC model, to a state-of-the-art, fully relativistic model [16], rendered a good description of the data. The authors concluded that the data favor models with a medium-modified form factor, but that the statistical significance was not sufficient to rule out calculations without form-factor modification.

A similar experiment, E93–049, was subsequently performed in Hall A at JLab [44, 45]. As this experiment was designed to detect differences between the in-medium polarizations compared to the free values, both ^{4}He and ^{1}H targets were employed (due to beam-time constraints, only ^{4}He data were acquired at $Q^2 = 2.6$ (GeV/c)^2). The statistical precision for the polarization double ratio was roughly 5.5%, 4.5%, 4.5%, and 10% at Q^2 of 0.5, 1.0, 1.6, and 2.6 (GeV/c)^2, respectively. The systematic uncertainty, predominantly due to uncertainties in the spin transport through the HRS spectrometer, is estimated to be 1.3% at $Q^2 = 1.0$ (GeV/c)^2.

The E93–049 results are shown in Fig. 6, for all four values of Q^2. The results are expressed in terms of the polarization double ratio

$$R = \frac{(P'_x/P'_z)_{^4\mathrm{He}}}{(P'_x/P'_z)_{^1\mathrm{H}}}. \tag{2}$$

Here, the helium polarization ratio is normalized to the hydrogen polarization ratio measured in the identical setting. Such a double ratio cancels nearly all systematic uncertainties. As a cross-check, the hydrogen results were also used to extract the free-proton form-factor ratio G_E/G_M, which was found to be in excellent agreement with previous data [26, 27]. In addition, the E93–049 result at $Q^2 = 0.5$ (GeV/c)^2 closely coincides with the recent results at $Q^2 = 0.4$ (GeV/c)^2 of Mainz [43], also shown in Fig. 6.

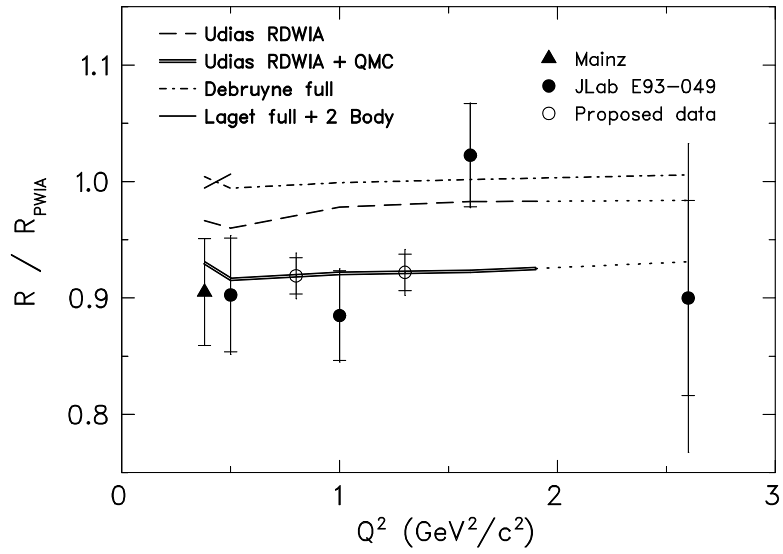

Figure 6: *Superratio R/R_{PWIA} as a function of Q^2 (closed circles). In PWIA the double polarization ratio, R_{PWIA}, is identically unity (barring acceptance-averaging effects). The dashed line shows the results of the full relativistic calculation of Udias et al. [16]. The dot-dashed line shows the results of the full nonrelativistic model of Debruyne et al. [49, 50]. The thin solid line shows the results of the full calculation, including two-body currents, of Laget [15]. The thick solid line indicates the full relativistic calculation of Udias [46] including medium modifications as predicted by a quark-meson coupling model [6]. For $Q^2 > 1.8$ (GeV/c)^2 the Udias calculations maintain a constant relativistic optical potential and are indicated as short-dashed lines. The lines connecting the acceptance-averaged theory calculations are to guide the eye only. The open circles indicate the projected data from this proposal.*

Table 1: *Statistical comparisons of the polarization double ratio R (see text) with various model calculations. The first entry is a Plane-Wave Impulse Approximation calculation only. The second entry is the full relativistic RDWIA calculation of Udias et al. [16]. The third entry incorporates [46] medium modifications to the latter, as predicted by a quark-meson coupling model [6]. The fourth entry is the full nonrelativistic model of Debruyne et al. [49, 50]. The last entry is a full nonrelativistic calculation of Laget including two-body currents [15] (only data up to Q^2 = 0.5 (GeV/c)^2 are taken into account).*

Model		χ^2/d.f.	d.f.	conf. level
Udias *et al.* (PWIA)	[16]	3.8	5	0.2%
Udias *et al.* (RDWIA)	[16]	2.2	5	5.4%
Udias *et al.* (RDWIA+QMC)	[16, 46]	1.3	5	26.3%
Debruyne *et al.* (Full)	[49, 50]	3.8	5	0.2%
Laget (Full + 2Body)	[15]	4.2	2	1.6%

The theoretical predictions are results of the acceptance-averaging of calculations by the Madrid group [16, 46]. We note that these relativistic calculations provide good descriptions of, e.g., the induced polarizations as measured at Bates in the ^{12}C(e,e$'\vec{p}$) reaction [47] and of A_{TL} in ^{16}O($\vec{e}, e'\vec{p}$) as previously measured at JLab [42].

At Q^2 = 0.5 and 1.0 (GeV/c)^2, the plane-wave impulse approximation (PWIA) calculation overestimates the data by $\approx 10\%$. The relativistic distorted-wave impulse approximation (RDWIA) calculation gives a slightly smaller ($\approx$ 3%) value of R but still overpredicts the data. The inclusion of a medium modification of the proton form factor as predicted by Lu *et al.* [6] in the RDWIA calculation is in excellent agreement with both settings. All calculations shown use the Coulomb gauge, the $cc1$ current operator as defined in [48], and the MRW optical potential of [31]. The $cc2$ current operator gives higher values of R, worsening agreement with the data. In general, various choices for, e.g., spinor distortions, current operators, and relativistic corrections affect the theoretical predictions by $\leq 3\%$, and presently can not explain the disagreement between the data and the RDWIA calculations.

A statistical analysis of the measured double ratios and various theoretical predictions was performed. Table 1 presents the χ^2 per degree of freedom and the confidence level of each calculation. It is obvious that the best description can be found for calculations that include medium modifications. In fact, calculations without such effects have a relatively small ($< 5\%$) confidence level, whereas the calculation with such effects has an appreciable ($\approx 26\%$) confidence level.

The E93–049 results, binned versus missing momentum, are shown in Fig. 7

for three of the four kinematical settings, along with theoretical results, again in terms of the polarization double ratio R. The statistics at the $Q^2 = 2.6$ (GeV/c)^2 kinematics are not sufficient to make a meaningful comparison with calculations. Hence, this highest Q^2 point has been omitted from Fig. 7. Negative values of missing momentum correspond to the recoiling nucleus having a momentum component antiparallel to the direction of the three-momentum transfer. Both the PWIA and the RDWIA can be seen to give a reasonable, but not perfect, description of the missing-momentum dependence found in the data. As in Fig. 6, the normalization difference between the RDWIA calculation and the data can be largely cured by including the QMC medium modifications.

One can argue that the case is not so clear for the $Q^2 = 1.6$ (GeV/c)^2 kinematics, and that the calculation without QMC medium modifications gives a satisfactory description of the data. This in essence mimics what can be seen in Fig. 6: The $Q^2 = 1.6$ (GeV/c)^2 data points lie generally above the calculation with QMC modifications. Still, the statistical analysis seems to indicate that this is merely a statistical fluctuation. Obviously, more precise data could settle this issue unambiguously, with high confidence level, and would constitute a demanding test of modern-day nucleon/meson descriptions of nuclear physics.

Lastly, we show in Fig. 8 the induced polarizations, P_y, corrected for (small) false asymmetries, as a function of missing momentum. These induced polarizations are identically zero in the absence of FSI effects (in the one-photon exchange approximation) and constitute a stringent test of various model calculations. One sees that the induced polarizations are small for all measured Q^2 values. The dashed and dot-dashed curves constitute RDWIA calculations by Udias *et al.* [16] with the MRW [31] and RLF [30] relativistic optical potentials. For the induced polarization case, the RDWIA curves with and without medium modifications are identical; the QMC model incorporates modifications only to the one-body form factors. For a rigorous calculation of the $^4\mathrm{He}(e, e'\vec{p})^3\mathrm{H}$ results presented here, one would need to take into account possible medium modifications to both one-body form factors and many-body FSI effects.

Figure 8 confirms the expected smallness of the induced polarizations, and seems to indicate a reasonable agreement with the RDWIA calculation of Udias *et al.* [16, 46]. This is important, as an imperfect knowledge of reaction-mechanism effects in the theoretical calculations of the $^4\mathrm{He}(\vec{e}, e'\vec{p})\,^3\mathrm{H}$ reaction should also show up as imperfect agreement with the induced polarizations. For example, an underestimate of reaction mechanism effects in the present calculation [46] may be due to the neglect of IC and the choice of what to include as MEC within the relativistic calculation.

A far more detailed check of whether reaction mechanism effects in the $^4\mathrm{He}(\vec{e}, e'\vec{p})\,^3\mathrm{H}$ reaction are fully understood is precluded by the systematic uncertainty of the induced polarizations: false asymmetries are typically checked with the $^1\mathrm{H}(\vec{e}, e'\vec{p})$ reaction, but the $^4\mathrm{He}(\vec{e}, e'\vec{p})\,^3\mathrm{H}$ reaction populates a different phase space in the proton spectrometer than the $^1\mathrm{H}(\vec{e}, e'\vec{p})$ reaction, and more careful checkout of the false asymmetries in the Focal-Plane Polarimeter (FPP) are required. Here, we plan to "scan" the angle of the proton spectrometer while taking $^1\mathrm{H}(\vec{e}, e'\vec{p})$ data, thus expanding the effective phase space

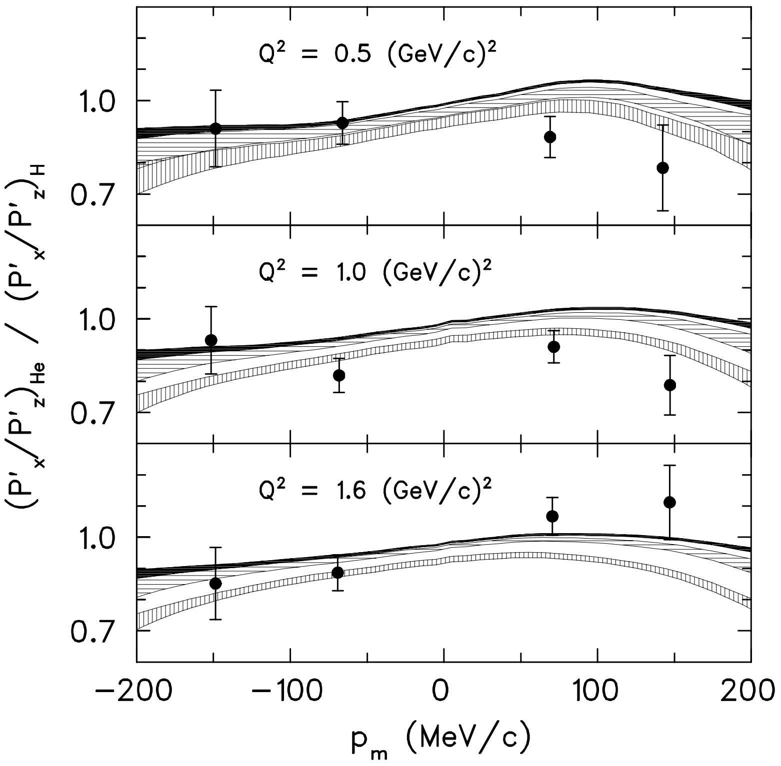

Figure 7: *Measured values of the polarization double ratio R_{Exp} for $^4He(\vec{e}, e'\vec{p})^3H$ at Q^2 = 0.5 $(GeV/c)^2$ (top), Q^2 = 1.0 $(GeV/c)^2$ (middle), and Q^2 = 1.6 $(GeV/c)^2$ (bottom). The shaded bands represent PWIA calculations (solid), relativistic DWIA calculations (horizontal dashes) and relativistic DWIA calculations including QMC medium–modified form factors [6] by Udias et al. [16] (vertical dashes). The bands take into account variations due to choice of current operator, optical potential, and bound-state wave function (see also Ref. [43]).*

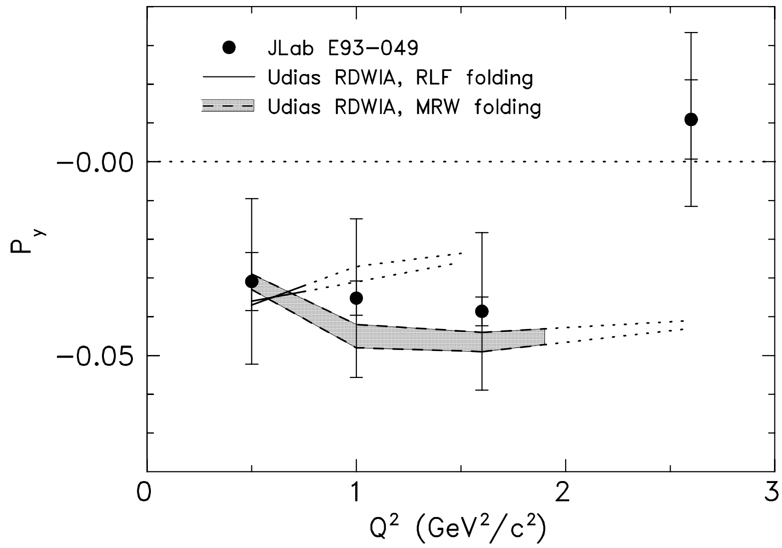

Figure 8: *Measured values of the induced polarizations for the* $^4He(\vec{e}, e'\vec{p})\,^3H$ *reaction. The inner uncertainty is statistical only, the total uncertainty includes a systematic uncertainty of* ± 0.02*, due to the imperfect knowledge of the false asymmetries. The dashed and dot-dashed curves show the results for the full relativistic calculations of Udias et al. [16, 46] with the MRW [31] and RLF [30] relativistic optical potentials used in the RDWIA calculations. All theoretical curves are averaged over the experimental acceptance.*

coverage with the Focal Plane Polarimeter.

3 The Proposed Experiment

3.1 Kinematics

In the proposed experiment we wish to improve on the precision of the polarization double ratio

$$R = \frac{(P'_x/P'_z)_{^4\mathrm{He}}}{(P'_x/P'_z)_{^1\mathrm{H}}}, \tag{3}$$

at $Q^2 = 0.8$ and 1.3 (GeV/c)^2. The expected statistical uncertainties, $\approx 1.7\%$, are of the same level as the systematic uncertainty, $\approx$1.3%, for the double ratio. The choice of four-momenta is motivated as follows:

- State-of-the-art RDWIA calculations are readily available and reliable in the proposed Q^2 region.
- Final-state interactions and other reaction mechanism effects are reduced as much as possible; in fact, the proposed kinematics combines all criteria to reduce FSI: quasielastic, parallel kinematics, low missing momentum, and symmetry about $\mathbf{p}_m = 0$.
- An extensive set of previous ^{16}O(e,e$'$p) data exists from Hall A experiments (E89-003, E89-033, and, more recently, E00-102) that forms a benchmark for RDWIA calculations at $Q^2 = 0.8$ (GeV/c)^2;
- A combination of better precession angle and higher rate allows for a significant improvement in figure-of-merit for a small decrease in Q^2 from E93-049's 1.6 (GeV/c)^2 to the proposed 1.3 (GeV/c)^2;

We chose electron beam energies to minimize the running times for a given uncertainty in the polarization double ratio. Note that this minimization technique is not very dependent on the exact choice of beam energy: there is a rather wide, shallow minimum around the quoted, standard beam energies. Kinematics are given in Table 2.

Compared to the previous E93–049 experiment, the statistical uncertainties here would be improved by over a factor of two. This would be accomplished by two measures:

- E93–049 used a beam current of 40 μA for the lower Q^2 values, combined with a beam polarization of $\approx$77%. Presently, the strained GaAs polarized source can deliver 100 μA of similarly polarized beam.
- E93–049 was approved for 12 days, and measured at four Q^2 values. This experiment would concentrate only at $Q^2 = 0.8$ and 1.3 (GeV/c)^2, at optimized beam energies. This minimizes the beam time needed to only 18 days.

Table 2: *Kinematics for the $^4He(e,e'p)^3H$ and $^1H(e,e'p)$ reaction.*

Q^2 $(\mathrm{GeV/c})^2$	Target	E_e (GeV)	$E_{e'}$ (GeV)	$\Theta_{e'}$ (deg)	p_p (GeV/c)	Θ_p (deg)
0.8	^{4}He	1.600	1.144	38.6	1.004	-45.3
	^{1}H	1.600	1.174	38.1	0.991	-47.0
1.3	^{4}He	2.400	1.672	33.1	1.353	-42.4
	^{1}H	2.400	1.707	32.7	1.334	-43.8

We also wish to improve on the precision of the induced polarizations, by mapping out the false asymmetries precisely, using the $^1\mathrm{H}(\vec{e}, e'\vec{p})$ reaction, while slightly varying the angle of the proton spectrometer. In this way, the recoiling protons scan over the full phase space of the Focal Plane Polarimeter. A precise knowledge of false asymmetries over the full detector would not only allow reduction of the overall systematic uncertainty of the acceptance averaged induced polarization to $0.01 - 0.02$, but, more importantly, would allow the study of the induced polarization as a function of various kinematical quantities (e.g., missing momentum or proton azimuthal angle).

3.2 Apparatus

The experiment is proposed for Hall A at Jefferson Lab. The experiment will make use of the two large-solid-angle high-resolution spectrometers (HRS). We intend to use the standard 10-cm long cryogenic helium and 15-cm long cryogenic hydrogen targets, and aluminum dummy targets for window subtraction. The proposed experiment will only employ the usual Hall A equipment. Both spectrometers will be equipped with their standard detector systems.

In essence, this is a rather simple experiment, where the main requirements are to run the $^4\mathrm{He}(\vec{e}, e'\vec{p})\,^3\mathrm{H}$ and $^1\mathrm{H}(\vec{e}, e'\vec{p})$ reactions back to back, and to add more data to minimize false asymmetries of relevance for the induced-polarization measurements.

3.3 Running Time Estimates

3.3.1 Backgrounds

Single rates from the (e, e'), (e, π^-), (e, p), and (e, π^+) reactions cause accidental coincidences which are a source of background for $^4\mathrm{He}(e, e'p)$. This background, however, was very low in the kinematics of experiment E93-049, and is expected to be much lower for the proposed experiment with more backward spectrometer angles. Background rate estimates are summarized in Table 3. The background

Table 3: *Estimated background rates for $^4He(e,e'p)$. Accidentals 100 ns are for accidentals into a 100-ns timing gate, including all particle types; 5 ns for accidentals into a 5-ns gate, including all particle types; 5 ns PID for accidentals into a 5-ns gate, including only e and p (assumes PID).*

	Singles (kHz)				Accidentals (Hz)		
Q^2	(e,e')	(e,π^-)	(e,p)	(e,π^+)	100 ns	5 ns	5 ns PID
0.8 $(\text{GeV/c})^2$	13	12	82	18	250	13	5.3
1.3 $(\text{GeV/c})^2$	4.8	17	85	26	240	12	2.0

is thus not expected to cause any problems in terms of particle identification (PID), the reals-to-accidentals ratio, or the data acquisition dead time.

3.3.2 Extraction of the polarizations

The physical quantities of interest, P'_x, P_y, and P'_z, will be determined by means of the maximum-likelihood technique, utilizing the azimuthal distribution of the protons scattered from the analyzer of the FPP.

$$I = I_0\left[1 + \epsilon_y \cos\varphi + \epsilon_x \sin\varphi\right] \tag{4}$$

The asymmetries ϵ_x and ϵ_y are proportional to the analyzing power for $\vec{p}+{}^{12}\mathrm{C}$ and to the proton's polarizations perpendicular to its momentum as it enters the analyzer. The measured asymmetries are linear functions of the proton's polarization components at the target. The linear relationship is given by a rotation which takes into account the change of coordinate system and the proton spin precession in the spectrometer's magnetic fields and is calculated on an event by event basis. For this we use a magnetic model of the spectrometer constrained by various optics data and "de-precess" using codes such as SNAKE [51] and COSY [52]. These models were studied in detail for the analysis of the G_E^p experiments E93-027 [26] and E99-007 [27]; see also the JLab technical note [55].

The absolute statistical uncertainties in the two accessible polarization components in the polarimeter frame P_x^{FPP} and P_y^{FPP} are [56]

$$\Delta P = \sqrt{\frac{2}{\bar{A}_c^2 \epsilon\, N_0}}, \tag{5}$$

where $\bar{A}_c$ is the analyzing power averaged over an angular cone for which A_c is substantially different from zero, ϵ is the fraction of events which scatter into this cone and N_0 is the total number of events detected in the spectrometer focal plane. Table 4 summarizes the assumed beam polarization h and the polarimeter and spin-transport parameters.

Table 4: *Assumed polarimeter- and spin-transport parameters. The values of* $\bar{A}_c$ *and* ϵ *are taken from [57]. Carbon indicates the assumed analyzer thicknesses.*

Q^2	$\bar{A}_c$	ϵ	h	χ	Carbon
0.8 $(\text{GeV/c})^2$	0.22	0.20	70%	118.1°	9″
1.3 $(\text{GeV/c})^2$	0.20	0.25	70%	141.5°	16.5″

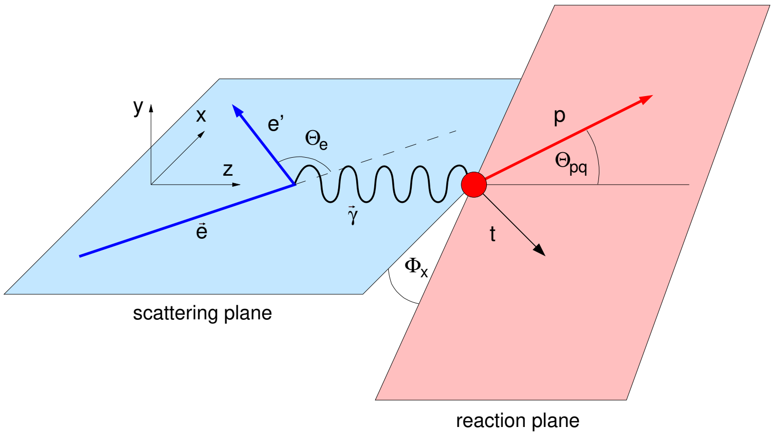

Figure 9: *Coordinate system used to define the components of the recoil proton polarization in the* $^4He(\vec{e}, e'\vec{p})\,^3H$ *reaction. The z axis is along the momentum transfer, the x axis is in the scattering plane perpendicular to the momentum transfer* $\vec{q}$ *and the y axis is perpendicular to the scattering plane, forming a right-handed system.*

3.3.3 Rate estimates

Rate estimates were done with the the Monte-Carlo code for electro nuclear coincidence experiments (MCEEP) [58]. The experiment requires a cryogenic target with 10-cm long ^{4}He and 15-cm long ^{1}H cells. The following limiting factors were included in the rate estimates:

- Maximum beam current of 100 μA.
- Maximum reasonable data acquisition rate is 3 kHz for coincidence experiments, with a dead time of 20% [59].
- VDC tracking efficiency of 80%.
- Fraction of events passing cuts in the FPP analysis, 70%.
- Event selection to guarantee elastic *ep* scattering or $p+{}^3$H final state (66%, and 58% respectively). These limits are in concordance with the E93-049 data.

We propose to obtain a 1.7% statistical uncertainty in the experimental ratio R, close to matching the systematic uncertainties in this ratio. This would constitute a decrease in the E93–049 uncertainties of over a factor of two. Our beam time estimates are given in Table 5.

Table 5: *Rate and beam time estimates, along with estimated statistical standard uncertainties for the polarization ratio* (P'_x/P'_z).

Q^2	Helium			Hydrogen		
	Rate	Time	stat. unc.	Rate	Time	stat. unc.
$(\mathrm{GeV/c})^2$	(Hz)	(h)	(%)	(Hz)	(h)	(%)
0.8	147	67	1.4	887	28	0.9
1.3	86	178	1.5	887	55	0.8

3.3.4 Systematic uncertainties

The main quantity of interest in this experiment is the polarization double ratio, $(P'_x/P'_z)_{\mathrm{He}}/(P'_x/P'_z)_{\mathrm{H}}$. In forming this quantity, systematic errors largely cancel (see Table 6 for an overview):

- The polarizations are ratio quantities reflecting a modulation of the φ-distribution relative to the flat, unpolarized baseline. Therefore, polarizations are relatively insensitive to luminosity, global detector efficiencies and spectrometer solid angles.
- The helicity-dependent polarizations are determined by taking differences of the φ-distributions for left and right beam helicities. This has the effect

Table 6: *Estimated systematic uncertainties for the polarization transfer double ratio,* $(P'_x/P'_z)_{\mathrm{He}}\,/(P'_x/P'_z)_{\mathrm{H}}$ *.*

Effect	uncertainty
Spin Transport	
— Proton trajectory	$< 1.5\%$
— Magnetic fields	$< 0.5\%$
Carbon Analyzing Power	0%
Electron Beam Polarization	0%

of canceling the instrumental asymmetries for the polarization transfer observables to first order.

- The ratio P'_x/P'_z is independent of the polarimeter analyzing power and the beam polarization.

- The only significant experimental systematic uncertainty in the determination of the polarization ratio is the determination of the spin precession in the spectrometer. There are two contributions to this uncertainty, one due to the knowledge of the initial proton trajectory, and the other due to the knowledge of the magnetic field of the spectrometer. The former part of the systematic uncertainty was estimated by introducing artificial shifts within the known spectrometer accuracy in various track parameters, and finding the effect on the ratio. The latter part was estimated for this proposal by Pentchev for the hydrogen polarization-transfer ratio P'_x/P'_z using the G_E^p data (E93-027 [53], E99-007 [54]) to be not larger than 0.8%. (For the detailed studies undertaken, see [55]). By further taking the ratio to the free case, $(P'_x/P'_z)_{\mathrm{He}}\,/(P'_x/P'_z)_{\mathrm{H}}$, the spin-precession errors partly cancel. However, there remains a residual error since the phase-space populations for helium and hydrogen targets are different.

The extraction of P_y will require a greater degree of understanding of the apparatus, especially with respect to instrumental uncertainties. From the E93-049 data, the systematic uncertainty in P_y is estimated to be ± 0.02. With dedicated ${}^1\mathrm{H}(e,e'\vec{p})$ elastic data, we hope to reduce this systematic uncertainty significantly in the proposed measurement.

4 Beam Time Request

The total beam time requested is 434 hours, or 18.1 days (see Table 7). Of these 18.1 days, 2.5 days are for mapping out the false asymmetries of the Focal Plane Polarimeter system using the ${}^1\mathrm{H}(\vec{e},e'\vec{p})$ reaction. Production data taking amounts to 13.7 days, split over the $Q^2 = 0.8$ and 1.3 (GeV/c)^2 kinematics ($\approx$ 4.0 and 9.7 days, respectively). Finally, the remaining time is dedicated to kinematics changes, beam polarization measurements, and to measurements of the target-wall background. The experiment will use beam energies of 1.60 GeV and 2.40 GeV, with two dedicated beam polarization measurements for each beam energy.

We require that the ${}^4\mathrm{He}(\vec{e},e'\vec{p})\,{}^3\mathrm{H}$ and ${}^1\mathrm{H}(\vec{e},e'\vec{p})$ reactions be run back to back in order to minimize systematic uncertainties, for both values of Q^2. The experiment requires a cryogenic target with 10 cm long ^{4}He and 15 cm long ^{1}H cells. Depending on scheduling, a few-day installation period may be needed to change the cryotarget configuration. No time is requested in the proposal for the changeover, since it may not be necessary.

We request a beam current of up to 100 μA, on both targets (40 μA for the Al "dummy" target), and a beam polarization of at least 70%.

A summary of the beam-time request is given in Table 7.

Table 7: *Summary of beam-time request.*

Target	Q^2 $(\mathrm{GeV/c})^2$	Purpose	Time (h)
He	0.8	Production	67
H	0.8	Production	28
H	0.8	False Asymmetries	24
Al	0.8	Wall subtraction	12
He	1.3	Production	178
H	1.3	Production	55
H	1.3	False Asymmetries	36
Al	1.3	Wall subtraction	12
—	—	Beam Energy Change (1)	8
—	—	Additional Spectrometer Changes (2)	2
—	—	Møller Measurements (4)	12
		Total	434

References

[1] S.A. Moszkowski and B.L. Scott, Ann. Phys. **11** (1960) 65.

[2] M. Sargsian *et al.*, J. Phys. G **29** (2003) R1.

[3] G. Miller, private communication (2003).

[4] W. Melnitchouk, K. Tsushima, A.W. Thomas, Eur. Phys. J. A **14** (2002) 105.

[5] A.W. Thomas, private communication (2003).

[6] D.H. Lu, K. Tsushima, A.W. Thomas, A.G. Williams and K. Saito, Phys. Lett. **B417** (1998) 217 and Phys. Rev. C **60** (1999) 068201.

[7] J. Jourdan, Phys. Lett. **B353** (1995) 189.

[8] J. Morgenstern and Z.-E. Meziani, Phys. Lett. **B515** (2001) 269.

[9] J. Carlson, J. Jourdan, R. Schiavilla, and I. Sick, Phys. Lett. **B553** (2003) 191.

[10] I. Sick, Comm. Nucl. Part. Phys. **18** (1988) 109.

[11] T.E.O. Ericson and A. Richter, Phys. Lett. **B183** (1987) 249.

[12] M.R. Frank, B.K. Jennings and G.A. Miller, Phys. Rev. C **54** (1996) 920.

[13] U.T. Yakhshiev, U-G. Meissner, and A. Wirzba, arXiv:nucl-th/0211055 (2002).

[14] H. Arenhövel, private communication (2003).

[15] J.-M. Laget, Nucl. Phys. **A579** (1994) 333.

[16] J.M. Udias *et al.*, Phys. Rev. Lett. **83** (1991) 5451; J.A. Caballero, T.W. Donnelly, E. Moya de Guerra and J.M. Udias, Nucl. Phys. **A632** (1998) 323; J.M. Udias and J.R. Vignote, Phys. Rev. C **62** (2000) 034302.

[17] J.J. Kelly, Phys. Rev. C **60** (1999) 044609.

[18] G. van der Steenhoven *et al.*, Phys. Rev. Lett. **57** (1986) 182; **58** (1987) 1727.

[19] P. Ulmer *et al.*, Phys. Rev. Lett. **59** (1987) 2259.

[20] D. Reffay-Pikeroen *et al.*, Phys. Rev. Lett. **60** (1988) 776.

[21] T.D. Cohen, J.W. Van Orden, and A. Picklesimer, Phys. Rev. Lett. **59** (1987) 1267.

[22] A. Magnon *et al.*, Phys. Lett. **B222** (1989) 352.

[23] J.E. Ducret *et al.*, Nucl. Phys. **A553** (1993) 697c.

[24] A.I. Akhiezer and M.P. Rekalo, Sov. J. Part. Nucl. **3** (1974) 277; R. Arnold, C. Carlson and F. Gross, Phys. Rev. C **23** (1981) 363.

[25] With the initial and final electron momentum $\vec{k}_i$ and $\vec{k}_f$, the coordinate system is given by the unit vectors $\hat{z} = (\vec{k}_i - \vec{k}_f)/|\vec{k}_i - \vec{k}_f|$, $\hat{y} = (\vec{k}_i \times \vec{k}_f)/|\vec{k}_i \times \vec{k}_f|$, and $\hat{x} = \hat{y} \times \hat{z}$.

[26] M.K. Jones *et al.*, Phys. Rev. Lett. **84** (2000) 1389.

[27] O. Gayou *et al.*, Phys. Rev. C **64** (2001) 038202.

[28] O. Gayou *et al.*, Phys. Rev. Lett. **88** (2002) 092301.

[29] Jefferson Lab experiment E93-049 *Polarization Transfer in the Reaction* $^4He(e,e'p)^3H$ *in the Quasi-elastic Scattering Region*, R. Ent and P. Ulmer, spokespersons.

[30] C. J. Horowitz, Phys. Rev. C **31** (1985) 1340.

[31] J.A. McNeil, L. Ray and S.J. Wallace, Phys. Rev. C **27** (1983) 2123.

[32] J.F.J. van den Brand *et al.*, Phys. Rev. Lett. **66** (1991) 409.

[33] R. Schiavilla, Phys. Rev. Lett. **65** (1990) 835.

[34] J.J. Kelly, Phys. Rev. C **59** (1999) 3256.

[35] A.Meucci, C.Giusti and F.D.Pacati, nucl-th/0205055.

[36] J.M. Laget, Nucl. Phys. A **579** (1994) 333.

[37] D. Eyl *et al.*, Z. Phys. A **352** (1995) 211.

[38] B.D. Milbrath, J. McIntyre *et al.*, Phys. Rev. Lett. **80**, (1998) 452.

[39] D.H. Barkhuff, *et al.*, Phys. Lett. B **470**, (1999) 39.

[40] Jefferson Lab experiment E89-028, *Polarization Transfer Measurements in the D(e,e'p)n Reaction*, M. Finn, M. Jones, and P. Ulmer spokespersons.

[41] H. Arenhövel, private communication.

[42] S. Malov *et al.*, Phys. Rev. C **62**, (2000) 057302.

[43] S. Dieterich *et al.*, Phys. Lett. **B500** (2001) 47.

[44] S. Dieterich, Ph.D. thesis, Rutgers University (2002).

[45] S. Strauch *et al.*, arXiv:nucl-ex/0211022, submitted to Phys. Rev. Lett. (2002).

[46] J. Udias, private communications.

[47] J. Gao *et al.*, Phys. Rev. Lett. **84** (2000) 3265.

[48] T. de Forest, Nucl. Phys. **A392** (1983) 232.

[49] J. Ryckebusch, D. Debruyne, W. Van Nespen and S. Janssen, Phys. Rev. C **60** (1999) 034604.

[50] D. Debruyne, Ph.D. thesis, University of Gent (2001).

[51] P. Vernin, SNAKE (private communication), SPhN-CEA in Saclay, France.

[52] M. Bertz, COSY INFINITY version 7, Michigan State University NSCL Technical Report MSUCL-977, 1995.

[53] Jefferson Lab experiment E93-027, *Electric Form Factor of the Proton by Recoil Polarization*, C. Perdrisat, and V. Punjabi, spokespersons.

[54] Jefferson Lab experiment E99-007, *Measurement of* G_{E_P}/G_{M_P} *to* $Q^2 = 5.6$ GeV^2 *by the Recoil Polarization Method*, E. Brash, M. Jones, C. Perdrisat, and V. Punjabi, spokespersons.

[55] L. Pentchev, J. LeRose, and the FPP collaboration, *Quadrupole alignment studies in the HRSs*, JLab-TN-01-052; see Technical Notes at `http://hallaweb.jlab.org/`.

[56] B. Bonin *et al.*, Nucl. Instr. Meth. **A288** (1990) 379.

[57] Hall-A status report, 2000; see Status Report Archive at `http://hallaweb.jlab.org/`.

[58] P. Ulmer, MCEEP, Monte Carlo for Electro-Nuclear Coincidence Experiments, Program Version 3.4 (2000).

[59] The increase of the data acquisition rate from about 2 kHz to 3 kHz with 20% deadtime was made possible by a recent reconfiguration of the data acquisition system, and usage of lower resolution TDCs. (R. Michaels, private communication).